JOURNAL OF Applied Polymer SCIENCE

Special Issue: Sustainable Polymers and Polymer Science Dedicated to the Life and Work of Richard P. Wool

Guest Editors: Dr Joseph F. Stanzione III (Rowan University, U.S.A.)
and Dr John J. La Scala (U.S. Army Research Laboratory, U.S.A.)

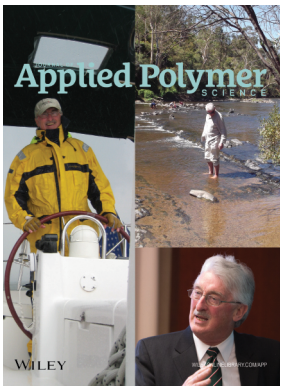

EDITORIAL

REVIEWS

RESEARCH ARTICLES

JOURNAL OF Applied Polymer SCIENCE

Special Issue: Sustainable Polymers and Polymer Science Dedicated to the Life and Work of Richard P. Wool

Guest Editors: Dr Joseph F. Stanzione III (Rowan University, U.S.A.)
and Dr John J. La Scala (U.S. Army Research Laboratory, U.S.A.)

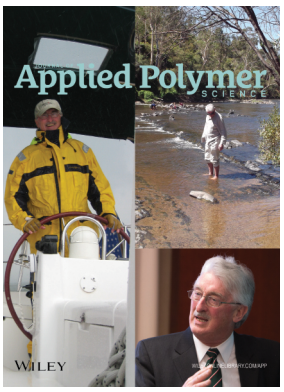

JOURNAL OF Applied Polymer SCIENCE

High surface area carbon black (BP-2000) as a reinforcing agent for poly[(−)-lactide]

Paula A. Delgado,[1] Jacob P. Brutman,[1] Kristina Masica,[1] Joseph Molde,[2] Brandon Wood,[2] Marc A. Hillmyer[1]

[1]Department of Chemistry, University of Minnesota, Minneapolis, Minnesota 55455
[2]Biotechnology Department, University of Minnesota, St. Paul, Minnesota 55108
Correspondence to: M. A. Hillmyer (E-mail: hillmyer@umn.edu)

ABSTRACT: The brittle nature and low-heat distortion resistance of a promising biorenewable thermoplastics, poly((−)-lactide) (PLA), motivate the investigation of strengthening additives that can address these deficiencies. In our work, a high surface area carbon black (BP-2000) as well as biobased carbon blacks (hydrochars) were examined as reinforcement agents for PLA. When 1–5 wt % BP-2000 was added to PLA, the crystallization of PLA was accelerated, resulting in higher crystallinity, tensile strength, and heat resistance. A thermal creep experiment revealed that the composites exhibited no significant deformation after 30 min with 2 N of uniaxial tensile force at 80 °C (above the T_g), whereas neat PLA (with similar thermal history) elongated to 79% after 5 min under the same conditions. PLA–hydrochar composites demonstrated similar brittle behavior to neat PLA. Despite the promising nucleating ability of hydrochars, they displayed low interfacial adhesion with PLA because of their low surface area, resulting in poor energy transfer on stretching. © 2016 Wiley Periodicals, Inc. J. Appl. Polym. Sci. **2016**, *133*, 43926.

KEYWORDS: blends; crystallization; polyesters; synthesis and processing

Received 4 January 2016; accepted 16 May 2016
DOI: 10.1002/app.43926

INTRODUCTION

Because of the high demand of polymeric materials for packaging and the environmental harm caused by the current industrial standard of petroleum-based materials, there is an urgent interest in finding green alternatives to polymeric materials for packaging.[1] To meet this demand, such alternatives must have comparable mechanical characteristics with their petroleum-based counterparts and be capable of degradation under controlled conditions.[2] Poly[(−)-lactide], PLA, is a biodegradable, hydrophobic, and aliphatic thermoplastic polyester and has proven to be a promising alternative to poly(styrene) (PS) or poly(ethylene terephthalate) (PET) because of its similar tensile strength, modulus, impact strength, and cost. However, the advantages of PLA have not yet been fully realized because of its brittle nature and low heat distortion temperature (50 °C) when compared with, for example, PET (115 °C).[2] One strategy to overcome these limitations has been to toughen of PLA through compatibilization with poly(ethylene), poly(glycolide), and poly(ε-caprolactone)[3–5] or plasticization with natural oils (such as castor and soybean oils).[6,7] Such rubbery domains have successfully increased the elongation at break of PLA but at the cost of decreasing the modulus and the tensile strength. Stereocomplexation between poly[(+)-lactide] and poly[(−)-lactide] has proven to be a successful alternative method toward increasing the melting temperature (T_m) from 160 to 220 °C, therefore decreasing the heat distortion of the material.[8] However, high enantiomeric purity of the two polymers is necessary to accomplish such a large increase in T_m. A more commercial approach to increasing the heat distortion and modulus of PLA is by reinforcement with high modulus materials such as glass fibers, cellulose, or flax.[9,10] These materials not only impart stiffness to the matrix but also induce a higher degree of crystallinity by acting as nucleating agents.

Alternative reinforcing materials such as carbon blacks (CBs) are usually produced from partial combustion or thermal decomposition of residual hydrocarbon materials.[11] Because of their high modulus, CBs have been used extensively to strengthen rubbers and thermoplastics. Specifically, CBs have been blended with PLA to serve as nucleating agents, conductive fillers, and compatibilizers for immiscible polymer blends.[11–18] The toughening capabilities of CBs depend highly on their intrinsic properties such as particle size, aggregate size, porosity, and surface chemistry.[19,20]

Additional Supporting Information may be found in the online version of this article.

The most common CBs to serve as fillers in a PLA matrix are CB3000 (SPC, Sweden),[11–13] Mogu-L (SPC, Sweden),[14] N-234 (Cabot, Boston, MA),[15–17] and VXC-605 (Cabot).[18] These materials, which typically have particle sizes between 24 and 134 nm and chemisorption surface areas (I_2) between 120 and 1000 mg g^{-1}, have successfully imparted an increase in the tensile strength of PLA, where they serve as nucleation agents, thus, decreasing the cold crystallization temperature (T_{cc}) of PLA. To the best of our knowledge, the highest surface area CB used to reinforce PLA was CB3000 (I_2: 1000 mg g^{-1}), which successfully increased the tensile strength of PLA from 36 to 57 MPa.[12,13]

Taking into consideration the strong interaction between the surfaces of the dispersed materials and the matrix material, we explored the reinforcing ability of one of the highest surface area CBs (Black Pearls 2000, BP-2000, I_2: 1494 mg g^{-1}; value obtained from Cabot Corporation). Furthermore, we investigate the PLA toughening capability of biobased hydrochars, produced from hydrothermal carbonization of biomass residuals.[21] In this study, we explore the enhancement of PLA crystallization, toughness, and thermal creep resistance by these carbon-based fillers, which we hypothesize is caused by enhanced nucleation effects.

EXPERIMENTAL

Materials

PLA was provided by NatureWorks (PLA 4032D, Minnetonka, MN, USA) with a number–average molar mass, M_n [size-exclusion chromatography (SEC), refractive index (RI), chloroform], of 91 kg mol^{-1} and dispersity, $Đ$, of 2.1. The concentration of (+)-isomer was 1.4%. Carbon Black BP-2000 was provided by Cabot. Hydrochars were obtained from the Biotechnology Institute at the University of Minnesota.[21] PLA, BP-2000, and hydrochars were dried under reduced pressure at room temperature prior to use.

Preparation of PLA/BP-2000 and PLA/Hydrochar Composites

Polymer blends were prepared using a recirculating, conical twin-screw extruder (DACA instrument, 4 g capacity) at 150 rpm and a temperature of 190 °C. The PLA was first melted for 5 min, after which BP-2000 or hydrochars were incorporated in 1–5 wt %. The blends were mixed for an additional 5 min before being collected. Dog-bone-shaped tensile bars [0.7 mm (T) × 3 mm (W) × 25 mm (L)] were obtained after press-molding the samples at 190 °C for 7 min and subsequently quenching at a rate of 10 or 40 °C min^{-1}. SEC confirmed that no significant degradation of PLA occurred at extrusion conditions as the M_n of PLA only changed from 91 to 88 kg mol^{-1} after blending the sample with BP-2000 at 190 °C for 10 min and from 88 to 86 kg mol^{-1} after press-molding the samples at 190 °C for 7 min.

Characterization

Size-exclusion chromatography (SEC) was performed at 35 °C on a Hewlett-Packard (Agilent Technologies) 1100 series liquid chromatograph equipped with a Hewlett-Packard 1047A RI detector. The instrument operates using three Plgel 5 μm Mixed-C columns in series with a molar mass range of 400–500,000 g mol^{-1}. Chloroform was used as the mobile phase with an elution rate of 1 mL min^{-1}. The samples were prepared by dissolving 1 mg of polymer in 1 mL of chloroform and filtered through a 0.2 μm Teflon filter. Polystyrene standards (Agilent Technologies) were used for calibration of molar mass. Scanning electron microscopy was performed on a Hitachi S900 with a cold-field emission gun. The instrument was operated using a 1.5 keV accelerating voltage. The samples were mounted on an aluminum sample holder shimmed with carbon tape followed by sputter coating with Au/Pd deposition using a VCR high-resolution indirect ion beam sputtering system. Differential scanning calorimetry analysis was conducted on a TA Discovery instrument (New Castle, DE) at a heating rate of 10 °C min^{-1} under N_2 atmosphere. The instrument was calibrated using indium as a standard. All samples (3–6 mg) were prepared in hermetically sealed pans and were run under a nitrogen purge with an empty pan as a reference. The first cycle was recorded at 10 °C min^{-1} to 200 °C from samples that were previously cooled at 10 or 40 °C min^{-1} after press-molding. The glass transition temperatures were obtained at the mid-point of each transition. The percent crystallinity was calculated using the following equation:[9]

$$X_c(\%) = \frac{100(\Delta H_m - \Delta H_{cc})}{\Delta H_m^o - W_p}, \quad (1)$$

where ΔH_m = enthalpy of melting (J g^{-1}), ΔH_{cc} = enthalpy of cold crystallization (J g^{-1}), $\Delta H_m{}^0$ = theoretical crystallization enthalpy of the 100% crystalline matrix (93.7 J g^{-1}), and W_p = weight fraction of PLA in the composite materials.[9]

The kinetics of isothermal crystallization from the melt were acquired as follows: first, the thermal history of the sample was erased by heating the sample from room temperature to 200 °C at a rate of 10 °C min^{-1} and annealing at 200 °C for 5 min. The sample was then quickly cooled to a specific crystallization temperature (T_i = 75, 78, or 80 °C) at a cooling rate of 80 °C min^{-1} and kept at this temperature for 60 min. The overall crystallization process was followed by tracking heat flow as a function of time. After completing the crystallization during the isothermal scans, the samples were heated from the crystallization temperature (T_i) to 200 °C at a heating rate of 10 °C min^{-1}. The melting temperature peak was acquired from this scan. The isothermal crystallization kinetics were obtained from the isothermal scans, as analyzed by the Avrami equation (2)[22]:

$$X(t) = 1 - \exp(-Zt^n) \quad (2)$$

where $X(t)$ is the percentage of relative crystallization, n is the Avrami index, and Z is the overall crystallization rate constant. Fitting was obtained with a relative conversion range of 3–20%. Using the values obtained for Z and n, the crystallization half-time was calculated using the following equation:

$$t_{1/2} = \left(\frac{\ln(2)}{Z}\right)^{1/n}, \quad (3)$$

The overall crystallization rate constant, Z, was converted to a normalized rate constant, k, using the following equation:[23]

$$k = Z^{1/n}, \quad (4)$$

Thermogravimetric analysis (TGA) was conducted on a Perkin-Elmer Diamond TG/DTA (Waltham, MA) at a heating rate of

20 °C min^{-1} under N_2. Nitrogen sorption isotherms were obtained on a Quantachrome Autosorb iQ^2-MP (Boynton Beach, FL) at the temperature of liquid nitrogen (−196 °C). Samples were loaded in 6-mm stems and degassed for 24 h at room temperature before measurement. Brunauer-Emmett-Teller (BET) specific surface areas were obtained from the adsorption branch over the relative pressure range $P/P_0 = 0.05$–0.35. Tensile testing was conducted using dog-bone-shaped bars with sample dimensions of 0.7 mm (T) × 3 mm (W) × 25 mm (L). The samples were wrapped in aluminum foil and aged for 48 h at 25 °C in a vial filled with dry DRIERITE. Tensile measurements were performed on a Shimadzu AGS-X tensile tester equipped with a 500 N load cell at 25 °C (uniaxial extension rate: 5.0 mm min^{-1}). Young's modulus and tensile toughness values were calculated using Trapezium software. Reported values and standard deviations are the average of five samples.

Fourier transformation infrared (FTIR) spectra were obtained at 4 cm^{-1} resolution with a Bruker Alpha-P Platinum FTIR spectrometer equipped with a platinum attenuated total reflectance (ATR) sampling module hosting a diamond crystal (single bounce). The software used for data collection and workup is OPUS 7.0.

Wide-angle X-ray scattering (WAXS) data were collected at the Advanced Photon Source (APS) at Argonne National Laboratories at the Sector 5-ID-D beamline. The beamline is maintained by the Dow-Northwestern-Dupont Collaborative Access Team (DND-CAT). The source produces X-rays with a wavelength of 0.7293 Å. The sample to detector distance was 201 mm to cover a q-range of 0.67–3.54 $Å^{-1}$. The 2D scattering patterns were collected on Roper CCD detector and were azimuthally integrated to 1D profiles of I versus q using the data reduction software FIT2D. Crystalline samples were cooled at 10 °C min^{-1} from the press-mold and stored at room temperature prior to data acquisition. X_c was estimated from WAXS by determining the baseline of the WAXS pattern and subsequently dividing the area of the crystalline diffraction peak through the baseline from the entire area under the entire curve through the baseline.

Dynamic mechanical thermal analysis (DMTA) was performed on the dog-bone-shaped films (ca. 0.7 mm × 3 mm × 25 mm) with an RSA-G2 analyzer (TA Instruments) in tension film mode at maximum strain of 0.05% and a frequency of 1 Hz. The samples were heated from 30 to 170 °C at a heating rate of 5 °C min^{-1}. The heat distortion experiments were performed using the RSA-G2 analyzer. The dog-bone-shaped samples, cooled at 10 °C min^{-1} from the press-mold, were placed in the rectangular geometry of the rheometer and heated to 80 °C for 15 min. After this time, 2 N of tensile force was applied, and the samples were held at this force for 30 min for blends with BP-2000 or 5 min for neat PLA (after this time, the neat PLA reached the maximum elongation of the instrument).

RESULTS AND DISCUSSION

CBs are particles usually produced by thermal cracking or thermal decomposition (1200–1900 °C) of residual hydrocarbons (e.g., gases, oils, or distillers) in a controlled process.[12,24] After thermal pyrolysis and other processing techniques, the resultant material is typically in the form of nanoparticles with sizes between 5 and 100 nm. However, aggregation and agglomeration can occur rapidly, forming a material with particle sizes in 10–100 μm ranges.

In this work, we used Black Pearls 2000 (BP-2000) as a CB to increase the tensile strength of PLA. Contrary to the other CBs previously used to reinforce PLA, BP-2000 has a high surface area (BET: 1228 m^2 g^{-1}; I_2: 1494 mg g^{-1}; value obtained from Cabot Corporation) and a pore size (Quenched Solid State Functional Theory kernel for N_2 on carbon: 26 nm) that should facilitate an increase in the polymer/CB interfacial interactions. This functionality is usually referred to as the surface chemistry of chemisorbed oxygen complexes (i.e., carboxylic acids, phenolic, quinonic, or lactonic groups) present in CBs. FTIR spectroscopy (Supporting Information Figure S2) of BP-2000 revealed —COOR (1740 and 1180 cm^{-1}) and C—O—C functional groups (1077 and 999 cm^{-1}) that can favorably interact with the ester functionality of PLA for better interfacial adhesion. We hypothesized that these advantageous interactions between functional groups combined with the extremely high surface area of BP-2000 would cause an increase in PLA/BP-2000 interactions, resulting in a large increase in tensile strength as well as increase in the thermal creep resistance.

To investigate the reinforcing effect of BP-2000 on PLA, composites with 1–5 wt % of BP-2000 were explored. The SEM micrographs of BP-2000 and the uniaxially stretched composite surfaces with different BP-2000 content are shown in Figure 1. These micrographs reveal that BP-2000 particles are present in an aggregated state. Once it is blended with PLA, BP-2000 particles (highlighted in white dotted circles) decreased significantly in size, possibly due to the shear force present during the extrusion process. Furthermore, the BP-2000/PLA interface is not sharp within the matrix, suggesting a good interfacial adhesion between BP-2000 and PLA, especially if more than 3 wt % is introduced into the matrix.

The use of CBs can induce nucleation, thus accelerating the crystallization process, which will likely affect the thermal and mechanical properties of the material.[15–17] The nonisothermal crystallization of PLA/BP-2000 composites from the melt, at different cooling rates (from 200 °C to 25 °C at 40 °C min^{-1} or 10 °C min^{-1}; Supporting Information Table S2 and Figure S4), showed that when the composites were rapidly cooled (40 °C min^{-1}), the cold-crystallization temperature (T_{cc}, measured in the heating ramp) was reduced from 129 to 102 °C and that the cold crystallization exotherm was widened on the addition of BP-2000. A decrease in T_{cc} would likely facilitate the growth of spherulites, favoring the formation of a stiffer, more crystalline material.[25] Furthermore, the reduction in T_{cc} caused by BP-2000 should allow for lower temperature processing conditions, mitigating thermal degradation during cold crystallization. When more than 4 wt % of BP-2000 was added, T_{cc} increased to 108 °C, possibly due to a decrease in the PLA mobility at high loadings, and was indicative of reduced nucleation efficiency.[24,26] At this cooling rate (40 °C min^{-1}), the glass

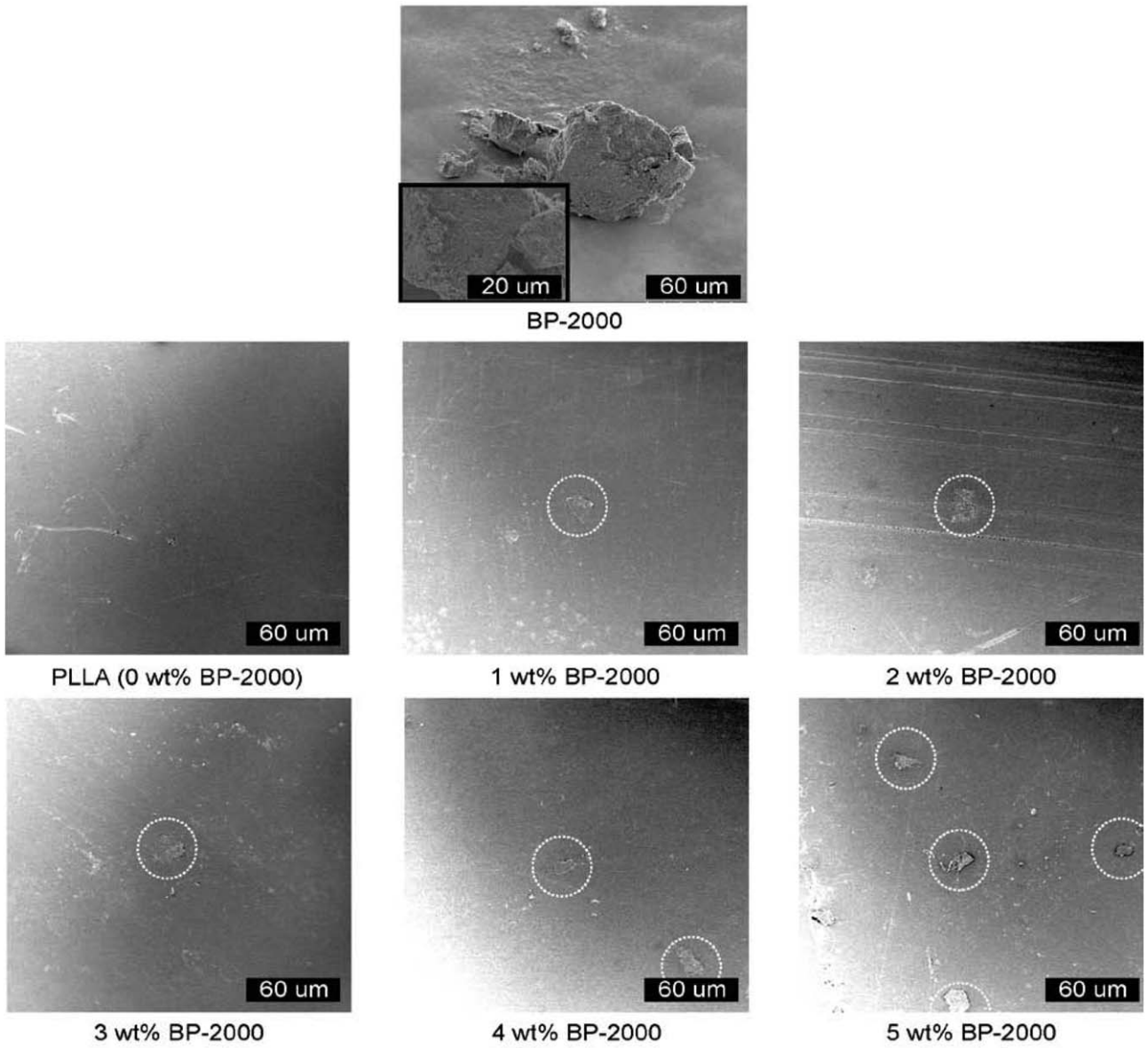

Figure 1. SEM micrographs of carbon black BP-2000 and the fracture surfaces of PLA/BP-2000 blends from 0 to 5 wt % BP-2000. Carbon black BP-2000 was dried at 100 °C under vacuum (20 mTorr) for 4 days, sprinkled over conductive tape and coated with Au/Pd before data acquisition. PLA/BP-2000 blends tensile bars were coated with Au/Pd before data acquisition. BP-2000 particles are highlighted in white-dotted circles within the PLA composites.

transition (T_g) and melting transition (T_m) temperatures were not affected by the incorporation of BP-2000 (Supporting Information Table S2). The two melting peaks at T_m observed for both the blends and neat PLA are referred to as the melting, recrystallization, and remelting process (reorganization mechanism), typical for crystalline polymers.[27] Consequently, a cooling rate of 40 °C min^{-1} was quite rapid, resulting in a lowered percent crystallinity of both the composites and neat PLA (X_c = 6.5–13.6%; Table I).

To facilitate the nucleating capability of BP-2000, the material was cooled at a slower rate (10 °C min^{-1}). These materials after this processing history generally exhibited a higher degree of crystallinity (X_c = 6–49%; Table I and Supporting Information Figure S4) and a higher T_g (64–66 °C), but no significant change on the T_m. The nucleation ability of BP-2000 was also followed by the change in the cold crystallization enthalpy (ΔH_{cc}) of the blends. At this cooling rate (10 °C min^{-1}), ΔH_{cc} decreased as more BP-2000 was added, until above 3 wt % BP-2000, the ΔH_{cc} was totally suppressed (Supporting Information Figure S4), that is, cooling these blends at 10 °C/min allowed them to fully crystallize corroborating the nucleating effect. The degree of crystallinity X_c, on the other hand, can be maximized at 3 wt % of BP-2000 addition, after which it begins to decrease. The crystallinity of these materials was also confirmed by WAXS (Supporting Information Figure S5) where the composites displayed the characteristic diffraction patterns of the α-form of the PLA at around 2θ = 14°, 16.6°, and 22.2°.[14]

Table I. Crystallinity of the PLA/BP-2000 with Respect to the Thermal History of the Material

	Degree of crystallinity, X_c (%)[a]			
BP-2000 (wt %)	Cooling at 40 °C min^{-1}[b]	Cooling at 10 °C min^{-1}[c]	Cooling at 10 °C min^{-1}[d]	After thermal annealing[e]
0	6.5	5.8	13.9	50.8
1	7.1	27.6	24.3	50.0
2	5.9	38.8	32.6	51.8
3	14.2	51.9	38.6	51.3
4	15.3	47.0	33.2	51.5
5	13.9	49.3	34.5	42.0

[a]Values calculated using eq. (1) from the differential scanning calorimetric thermograms using a heating rate of 10 °C min^{-1}.
[b]Data acquired from the first cycle where samples were cooled from the melt (190 °C) at 40 °C min^{-1} and aged for 48 h at 25 °C prior data acquisition.
[c]Data acquired from the first cycle where samples were cooled from the melt (190 °C) at 10 °C min^{-1} and aged for 48 h at 25 °C prior data acquisition.
[d]Data acquired from the first cycle where samples were cooled from the melt (190 °C) at 10 °C min^{-1} and aged for 48 h at 25 °C prior data acquisition except extracted from WAXS data in Supporting Information Figure S5.
[e]Data acquired from the second heating cycle after quenching the sample from the melt (190 °C) at 80 °C min^{-1} and annealing at 80 °C for 60 min.

To maximize X_c, neat PLA and the composites were annealed at 80 °C for 60 min (Table I). Interestingly, after thermal annealing of neat PLA and the composites, all samples exhibited similar X_c; combined with the previous results, this implies that BP-2000 significantly accelerates the crystallization of PLA and allows for the maximum degree of crystallinity to be achieved. Consequently, the composites should have smaller spherulites than neat annealed PLA, which have been shown to improve the mechanical properties of polymeric materials in prior studies.[24,25] Therefore, processing time should be substantially reduced for PLA when blended with BP-2000 due to the enhanced nucleation. This concept, when combined with a lower T_{cc}, reveals that blending PLA with BP-2000 is an attractive method for the production of PLA with shortened processing times at lower temperatures.

The Avrami equation is usually used to analyze the isothermal crystallization kinetics of a semicrystalline polymer [eqs. (2)–(4)].[22,23,28–30] In this case, the isothermal melt crystallization of PLA was studied by quenching the composites from the melt at a rate of 80 °C min^{-1} to a temperature below T_m (T_i) and annealed at this temperature for 60 min. From the crystallization exotherm, the overall crystallization rate constant (Z), the normalized rate constant (k), half-time of the crystallization ($t_{1/2}$), and the Avrami index (n) were calculated at T_i (from 75 to 80 °C; Table II). The n values ranged from 2.1 to 2.6, which suggest that spherulites grow with simultaneous nuclei formation or that axialites (two-dimensional aggregates) grow with nuclei formation over time.[25] Additionally, the higher crystallization rate constant and lower $t_{1/2}$ of these composites suggest that faster crystallization kinetics (when compared with neat PLA) is likely due to the nucleation effect from BP-2000 which increases the number of crystallization sites.[24,25] We evaluated the $t_{1/2}$, which is an important parameter for injection molding and industrial processing of semicrystalline materials.[25] Table II shows that the $t_{1/2}$ for the series of composites significantly decreased from 4–5 min to 2–3 min by a small change in T_i from 75 to 80 °C. More importantly,

Table II. Avrami Parameters for the PLA/BP-2000 Blends

Sample	T_i = 75 °C			T_i = 78 °C			T_i = 80 °C		
BP-2000 (wt %)	n	k 10^{-1} (min^{-1})	$t_{1/2}$ (min)	n	k 10^{-1} (min^{-1})	$t_{1/2}$ (min)	n	k 10^{-1} (min^{-1})	$t_{1/2}$ (min)
0							1.7	0.81	9.3
1	2.1	1.4	5.3	2.5	2.4	3.3	2.2	2.4	3.4
2	2.3	1.8	6.0	2.6	2.3	3.4	2.6	3.0	3.5
3	2.4	2.0	4.1	2.5	2.6	2.4	2.2	2.3	2.3
4	2.3	1.9	4.2	2.3	2.3	2.6	2.2	2.3	2.3
5	2.0	1.4	5.0	2.2	2.1	3.2	2.2	2.1	3.8

Data were acquired from the isothermal scans after erasing thermal history and quenching the sample at 80 °C min^{-1} from 190 °C to the specified temperature. T_i = isothermal crystallization temperature; n = Avrami index; k = normalized crystallization rate constant; $t_{1/2}$ = half-crystallization time; ρ_c = 1.359 (g cm^{-3}); and ρ_l = 1.25 (g cm^{-3}).

Table III. Mechanical Properties of PLA/BP-2000 Polymer Blends

	Cooling at 40 °C min^{-1}			Cooling at 10 °C min^{-1}		
BP-2000 (wt %)	ε_b (%)	σ_{TS} (MPa)	E (GPa)	ε_b (%)	σ_{TS} (MPa)	E (GPa)
0	3.2 ± 0.5	57 ± 5	2.1 ± 0.2	4.2 ± 0.6	58 ± 8	2.2 ± 0.2
1	3.4 ± 1.2	57 ± 5	2.2 ± 0.2	4.1 ± 0.9	64 ± 4	2.2 ± 0.1
2	2.9 ± 0.7	54 ± 10	2.1 ± 0.2	3.2 ± 1.1	64 ± 11	2.2 ± 0.2
3	3.2 ± 0.2	65 ± 3	2.2 ± 0.1	3.5 ± 0.1	70 ± 5	2.3 ± 0.1
4	3.6 ± 0.4	63 ± 7	2.2 ± 0.1	3.0 ± 0.4	67 ± 6	2.3 ± 0.1
5	3.1 ± 0.3	64 ± 5	2.2 ± 0.1	3.9 ± 0.1	67 ± 3	2.2 ± 0.1

Average values for samples were aged 48 h at 25 °C. Samples were cooled after press-molding from the melt at the determined cooling rate.

$t_{1/2}$ significantly reduced from 9 min to 3 min (at 80 °C) for neat PLA and PLA containing 1 wt % of BP-2000, respectively. This result further demonstrated the effectiveness of BP-2000 to nucleate the crystallization of PLA.

Uniaxial tensile tests were performed to investigate the mechanical properties of the PLA/BP-2000 composites prepared at both cooling rates, which yielded materials with different degrees of crystallinity. The elongation at break (ε_b), tensile strength (σ_{TS}), and modulus (E) of the composites are summarized in Table III. At a fast cooling rate (40 °C min^{-1}), the tensile strength slightly increased as the amount of BP-2000 increased. When the materials were cooled at 10 °C min^{-1}, the effect of the reinforcing agent is significantly more noticeable, leading to stiffer materials with the average σ_{TS} up to 10 MPa higher. In particular, the average σ_{TS} of neat PLA increases only 1 MPa, whereas the average σ_{TS} of the composite with 2 wt % BP-2000 increases by 10 MPa at the slower cooling rate. Remarkably, the incorporation of 3 wt % BP-2000 leads to an overall increase of 12 MPa in the average σ_{TS} when compared with that of neat PLA at a 10 °C min^{-1} cooling rate. This strengthening effect is likely due to an increase in the crystalline domains.[31,32]

To evaluate the thermal resistance of the composites, we performed DMTA on both neat PLA and the PLA/BP-2000 composites. This allowed us to follow the storage modulus as a function of the temperature [Figure 2(a,b)]. In the glassy regime (30–50 °C), the modulus of PLA is only slightly affected by the presence of the BP-2000. Beyond the glassy regime (>60 °C), the storage modulus drops as it passes through the T_g and increases again on reaching the cold-crystallization temperature (T_{cc}). Taking into account that the decrease in modulus and the T_{cc} depend highly on the degree of crystallization of the material (X_c), when PLA and PLA/BP-2000 composites were cooled at 10 °C min^{-1} [higher crystallinity; Figure 2(a)], the storage modulus of neat PLA dropped two orders of magnitude after passing the T_g (between 60 and 90 °C). In contrast, the storage modulus of the PLA/BP-2000 composites barely changed over this temperature range because of their higher degree of crystallinity (Table I), which confirms the ability of BP-2000 to accelerate the crystallization of PLA. This signifies that the material will deform less and therefore exhibit an increase in its operational temperatures.

The reinforcing nature of BP-2000 in PLA without the influence of the crystallization was explored by quenching with liquid N_2

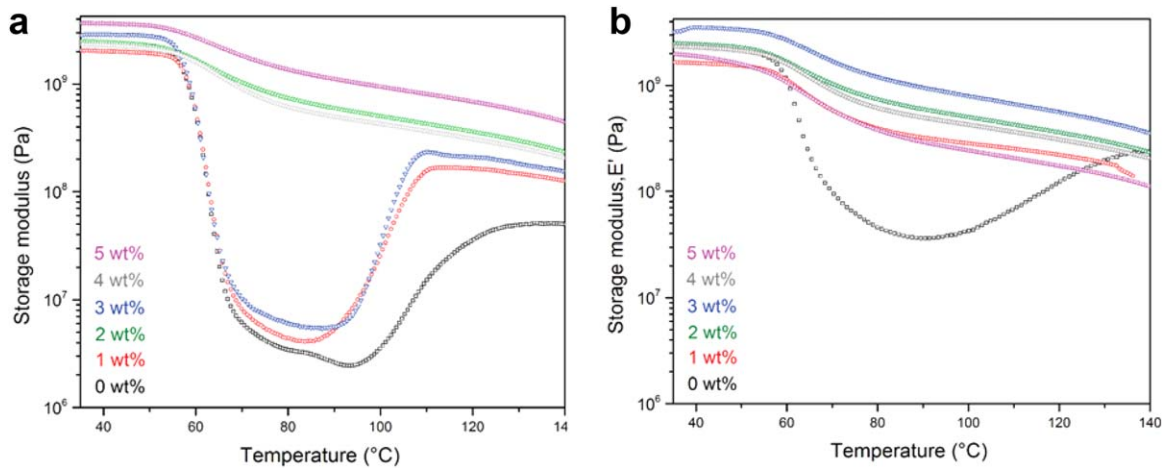

Figure 2. Dynamic mechanical thermal analysis of PLA/BP-2000 blends. Data were acquired at 6.28 rad s^{-1}, 0.05% strain, and at 5 °C min^{-1} after tensile deformation. (a) Samples were cooled at 10 °C min^{-1} and aged at 25 °C for 48 h. b) Samples were quenched with liquid N_2 from the melt and immediately measured. [Color figure can be viewed in the online issue, which is available at wileyonlinelibrary.com.]

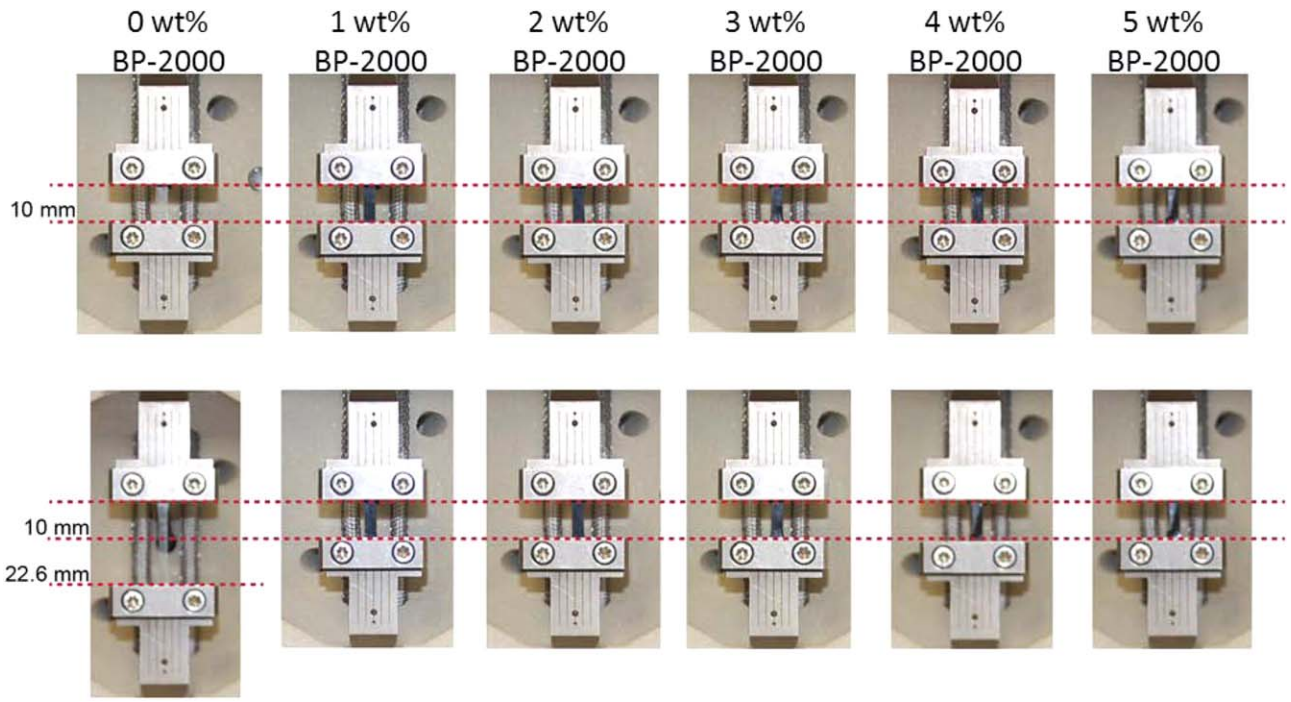

Figure 3. Thermal deformation experiment. Samples were held at a constant force of 200 g at 80 °C from 0 to 30 min. Before the experiment, samples were cooled at 10 °C min^{-1} from the melt and aged at 25 °C for 48 h. After 5 min, the neat PLA sample had deformed to the maximum elongation of the instrument, whereas the BP-2000 composites remained unchanged after 30 min. [Color figure can be viewed in the online issue, which is available at wileyonlinelibrary.com.]

on hot pressing; this should inhibit crystallization, thus resulting in a highly amorphous material. As shown in Figure 2(b), composites with 1 and 3 wt % of BP-2000 exhibited similar amorphous behavior to neat PLA, with a decrease of three decades on the storage modulus between 60 and 90 °C. A comparable storage modulus at this fast quenching implies that the amorphous composites did not exhibit any significant reinforcing effect from BP-2000. This suggests that the reinforcement comes from the ability of BP-2000 to nucleate the crystallization of PLA and not from the mechanical restraint imparted from its particles.[33] However, as the crystallization of the composites occurs very fast, we were not able to obtain amorphous materials with 2, 4, and 5 wt % BP-2000 loadings.

To demonstrate the usefulness of these results in PLA applications, a thermal deformation experiment was performed (Figure 3). In this case, samples with higher crystallinity (cooling rate: 10 °C min^{-1}; Table I) were placed in a rheometer and heated to 80 °C (ca. 10 to 20 °C above their T_g values). When the temperature was equilibrated, 2 N of constant uniaxial tensile force was applied. When neat PLA was studied, it elongated 79% after just 5 min, reaching the rheometer's maximum elongation. Remarkably, the PLA/BP-2000 composites did not show significant deformation after showing almost no creep after 30 min, indicating that these materials offer a facile method for producing PLA useful for high-temperature applications. We hypothesize that this thermal creep resistance is due to the strong interfacial adhesion between BP-2000 and PLA, thus, preventing the material from flowing above the T_g.

Alternative Carbon Blacks from Biomass

CBs from biomass, that is, animal manure and alcoholic fermentation byproducts also known as condensed distillers solubles (CDS) were also explored. In this study, the CBs were produced by the hydrothermal carbonization process (HTC), where the biomass is thermochemically decomposed by heating (200–250 °C) in the absence of oxygen and in the presence of water.[21,34,35] Products from HTC, known as hydrochars, contain high carbon content, making them suitable to be used as strengthening additives in PLA. In this work, hydrochars derived from dairy, CDS, swine, and poultry were used as reinforcement agents in PLA composites. The hydrochars used with their respective thermal treatment and nomenclature are summarized in Supporting Information Table S4.

The composition, functionality, particle size, and surface area of hydrochars were characterized by elemental analysis, ATR-FTIR spectroscopy, SEM, and N_2 sorption techniques (Supporting Information Figures S6–S25 and Tables S6–S10). Selected hydrochars from CDS, dairy, and poultry were blended at 3 wt % in PLA (Supporting Information Table S6). Supporting Information Table S7 summarizes the mean and standard deviation values of the mechanical performance of this series of PLA composites. Although the elongation at break and modulus were similar to neat PLA, a significant decrease on the tensile strength was observed for the majority of samples with the notable exception of swine hydrochar, HC2-S (see Supporting Information), which increased the average tensile strength of PLA by 4.2 MPa. This reduction in mechanical performance suggests a poor interfacial adhesion between PLA and the

hydrochars, which correlates to a poor stress transfer across the interface.[34] We attribute the poor interfacial adhesion to the significantly lower surface area of the hydrochars (BET = 5–23 $m^2\ g^{-1}$) versus BP-2000 (BET = 1228 $m^2\ g^{-1}$). The presence of voids (not observed on the BP-2000 composites) around the hydrochars from CDS [Supporting Information Figure S10(b,c)] is also evidence of the poor adhesion. However, the hydrochars were found to effectively accelerate the crystallization process of PLA, as the T_{cc} decreases about 30 °C (Supporting Information Table S6 and Figure S11) with 3 wt % of hydrochars in the composite. This increase in crystallization results in stiffer materials (evidenced by DMTA; Supporting Information Figure S12), as some of the composites exhibit a higher storage modulus in the glassy regime, and improved thermal properties as less deformation occurs at temperatures below 90 °C. Thermal creep resistance experiments were performed on the PLA–hydrochar composites; however, the brittle nature of the materials prevented data from being obtained.

CONCLUSIONS

We have shown that the use of high surface area carbon black (BP-2000) as well as biobased carbon blacks (hydrochars) allows for thermal reinforcement of PLA composites. When 1–5 wt % of BP-2000 was added to PLA, the composites showed a decrease in the T_{cc} (20 °C lower than neat PLA) that resulted in higher crystallinity, stiffer, stronger, and more thermally stable composite materials. DMTA experiments on crystallized and quenched amorphous materials revealed the ability of BP-2000 and hydrochars to rapidly accelerate the cold crystallization of PLA as well as its ability to induce high creep resistance. The high creep resistance was further confirmed through thermal creep experiments, which revealed that no significant deformation was observed at 2 N of force at 80 °C, contrary to the high elongation of neat PLA ($\varepsilon_b = 79\%$) after 5 min under same conditions. These results confirm an enhancement of the thermal stability of the composites, which could broaden the applications of PLA. When hydrochars were used as reinforcing agents, the resulting composites presented similar brittle behavior as neat PLA. Despite the promising nucleating ability of these materials, they displayed low surface area and thus low interfacial adhesion with PLA which resulted in brittle materials.

ACKNOWLEDGMENTS

This work was funded by the Biotechnology Department at the University of Minnesota and from partial support by the NSF under the Center for Sustainable Polymers, CHE-1413862. Part of this work was carried out at the Institute of Technology Characterization Facility, University of Minnesota, a member of the NSF-funded Materials Research Facilities Network. WAXS data were acquired at the DuPont-Northwestern-Dow Collaborative Access Team (DND-CAT) located at Sector 5 of the Advanced Photon Source (APS). DND-CAT is supported by E. I. Dupont de Nemours and Co., The Dow Chemical Co., and the State of Illinois. The use of APS was supported by the U.S. Department of Energy, Office of Science, Office of Basic Energy Sciences under contract no. DE-AC02-06CH11357. The authors thank Stacey Saba for her guidance on the nitrogen sorption experiments, Alejandro Müller and Arnaldo Lorenzo for providing the Avrami script, and Steven Heilmann for helpful discussions and project coordination.

REFERENCES

1. Wool, R. P.; Sun, X. S. In Bio-Based Polymers and Composites; Wool, R. P.; Sun, X. S., Eds.; Academic Press: Burlington, **2005**.
2. Grossman, R.; Nwabunma, D. In Poly(lactic acid): Synthesis, Structures, Properties, Processing, and Applications; Auras, R.; Lim, L.; Selke, S.; Tsuji, H., Eds.; Wiley: New Jersey, **2010**.
3. Jacobsen, S.; Fritz, H. G. *Polym. Eng. Sci.* **1999**, *39*, 1303.
4. Anderson, K. S.; Schreck, K. M.; Hillmyer, M. A. *Polym. Rev.* **2008**, *48*, 85.
5. Cabedo, L.; Feijoo, J. L.; Villanueva, M. P. *Macromol. Symp.* **2006**, *233*, 191.
6. Robertson, M. L.; Paxton, J. M.; Hillmyer, M. A. *ACS Appl. Mater. Interfaces* **2011**, *3*, 3402.
7. Gramlich, W. M.; Robertson, M. L.; Hillmyer, M. A. *Macromolecules* **2010**, *43*, 2313.
8. Tsuji, H.; Tezuka, Y. *Biomacromolecules* **2004**, *5*, 1181.
9. Wootthikanokkhan, J.; Cheachun, T.; Sombatsompop, N.; Thumsorn, S.; Kaabbuathong, N.; Wongta, N.; Wong-On, J.; Isarankura Na Ayutthaya, S.; Kositchaiyong, A. *J. Appl. Polym. Sci.* **2013**, *129*, 215.
10. Mohanty, A. K.; Misra, M.; Drzal, L. T. Natural Fibers, Biopolymers, and Biocomposites; CRC Press: Boca Raton, FL, **2005**.
11. Yu, J.; Wang, N.; Ma, X. *Biomacromolecules* **2008**, *9*, 1050.
12. Zhijun, Q.; Xingxiang, Z.; Ning, W.; Jianming, F. *Polym. Compos.* **2009**, *30*, 1576.
13. Ning, W.; Xingxiang, Z.; Jiugao, Y.; Jianming, F. *Polym. Int.* **2008**, *57*, 1027.
14. Su, Z.; Huang, K.; Lin, M. *J. Macromol. Sci. B: Phys.* **2012**, *51*, 1475.
15. Su, Z.; Li, Q.; Liu, Y.; Guo, W.; Wu, C. *Polym. Eng. Sci.* **2010**, *50*, 1658.
16. Su, Z.; Guo, W.; Liu, Y.; Li, Q.; Wu, C. *Polym. Bull.* **2009**, *62*, 629.
17. Su, Z.; Li, Q.; Liu, Y.; Hu, G.; Wu, C. *J. Polym. Sci. Part B: Polym. Phys.* **2009**, *47*, 1971.
18. Li, K.; Dai, K.; Xu, X.; Zheng, G.; Liu, C.; Chen, J.; Shen, C. *Colloid Polym. Sci.* **2013**, *291*, 2871.
19. Pritchard, G. In Plastic Additives: An A–Z Reference; Accorsi, J.; Yu, M., Eds.; Chapman and Hall: London, **1998**; pp. 153.
20. Pandolfo, A. G.; Hollenkamp, A. F. *J. Power Sources* **2006**, *157*, 11.
21. Wood, B.; Jader, L.; Schendel, F.; Hahn, N.; Valentas, K.; McNamara, P.; Novak, P.; Heilmann, S. *Biotechnol. Bioeng.* **2013**, *110*, 2624.
22. Lorenzo, A.; Arnal, M. L.; Albuerne, J.; Müller, A. *J. Polym. Test.* **2007**, *26*, 222.

23. Urbanovici, E.; Schneider, H. A.; Cantow, H. J. *J. Polym. Sci. Part B: Polym. Phys.* **1997**, *35*, 359.
24. Donnet, J. B.; Bansal, R. C.; Wang M. J., *Carbon Black Science and Technology*, 2nd ed.; Marcel Dekker: New York, **1993**.
25. Saeidlou, S.; Huneault, M. A.; Li, H.; Park, C. *Prog. Polym. Sci.* **2012**, *37*, 1657.
26. Kolstad, J. *J. Appl. Polym. Sci.* **1996**, *62*, 1079.
27. Su, Z.; Liu, Y.; Guo, W.; Li, Q.; Chifei, W. *J. Macromol. Sci. B: Phys.* **2009**, *48*, 670.
28. Anderson, K. S.; Hillmyer, M. A. *Polymer* **2006**, *47*, 2030.
29. Schmidt, S. C.; Hillmyer, M. A. *J. Polym. Sci. Part B: Phys* **2001**, *39*, 300.
30. Castillo, R. V.; Müller, A. J.; Raquez, J.-M.; Dubois, P. *Macromolecules* **2010**, *43*, 4149.
31. Mathew, A. P.; Oksman, K.; Sain, M. *J. Appl. Polym. Sci.* **2005**, *97*, 2014.
32. Perego, G.; Cella, G. D.; Bastioli, C. *J. Appl. Polym. Sci.* **1996**, *59*, 37.
33. Zhao, Y.; Cheung, H.; Lau, K.; Xu, C.; Zhao, D.; Li, H. *Polym. Degrad. Stabil.* **2010**, *95*, 1978.
34. Liu, W. J.; Jiang, H.; Yu, H. Q. *Chem. Rev.* **2015**, *115*, 12251.
35. Libra, J. A.; Ro, K.; Kammann, C.; Funke, A.; Berge, N.; Neubauer, Y.; Titirici, M.; Fühner, C.; Bens, O.; Kern, J.; Emmerich, K. *Biofuels* **2011**, *2*, 89.